Using subsurface geophysical methods in flood control: A resistivity survey to define underground storage capacity of a sand body in Ciudad Juárez, Mexico

Oscar S. Dena O.*, Griselda Obeso C., Diane Doser, Jesús E. Leyva, E. Rascon, Francisco Gómez and Miguel Domínguez A.

Resumen

En una zona localizada al sur de Ciudad Juárez, Chihuahua, que presenta serios problemas de inundación durante la época de lluvias, se llevó a cabo un estudio geoeléctrico de corriente directa, con el objetivo de determinar y evaluar la capacidad de almacenamiento de un estrato subyacente de arenas permeables, para prevenir inundaciones en "El Barreal", el cual se caracteriza por la presencia de naves industriales y desarrollos urbanos de tipo de interés social. En julio del 2008, eventos hidrometeorológicos intensos registraron 68 mm de precipitación en 24 horas, y un acumulado mensual de 146 mm, el cual representa casi el 50% de la precipitación anual media en Ciudad Juárez. Tales niveles de intensidad de precipitación ocasionaron inundaciones en gran parte de la superficie de la laguna "El Barreal", dejando cientos de casas y parques industriales anegados durante la contingencia. Un total de 9 Sondeos Eléctricos Verticales (SEV) se realizaron utilizando el arreglo Schlumberger para generar un modelo geológico. Dos zanjas exploratorias se excavaron para calibrar el método y realizar pruebas de permeabilidad. El método exitosamente diferenció las unidades estratigráficas de grano fino (limos y arcillas) y de grano grueso (arenas), para así inferir la presencia y geometría de cuerpos de arena permeable capaces de almacenar y transportar parte del volumen de los escurrimientos al acuífero, y funcionar así como una estrategia de mitigación para inundaciones en la zona de "El Barreal". Por lo tanto, el implementar una batería o red de pozos de infiltración, localizados estratégicamente en la parte oeste del sistema lagunar y diseñados para alcanzar profundidades mayores a los 12 m, es una solución ingenieril práctica y factible para parcialmente resolver los problemas de inundación en la parte baja de la cuenca el Barreal.

Palabras clave: runoff, flooding, hydrology, VES, permeability, infiltration.

Abstract

A DC resistivity survey was conducted over a flood prone area (playa lake) in the southern urbanized area of Ciudad Juárez, Chihuahua, Mexico to locate and evaluate the water storage capacity of a subsurface permeable sand stratum to prevent flooding "El Barreal", a large urban area of housing developments and industrial compounds. Recent major floods in July 2008 record were caused by precipitation levels of 68 mm in 24 hours, and a monthly accumulation of 146 mm. Hundreds of homes and industrial enterprises were flooded. Nine vertical electrical soundings (VES) were conducted utilizing a Schlumberger array to generate a geologic model. Two trenches were excavated to calibrated the method and perform permeability tests. The method successfully discriminated between fine grained clay and silt and coarse sand. The subsurface sand body will be used as a temporary storage facility for flood control during summer storms amounting to up to half the total annual rainfall.

Key words: escurrimiento, inundación, hidrología, SEV, permeabilidad, infiltración.

O.S. Dena O.*
G. Obeso C.
J. E. Leyva
M. Domínguez A.
Instituto de Ingeniería y Tecnología
Universidad Autónoma de Ciudad Juárez
*Corresponding author: osdena@gmail.com

E. Rascon
F. Gómez
Junta Municipal de Aguas y Saneamiento

D. Doser
Departament of Geological Sciences
University of Texas at El Paso

O. S. Dena O., G. Obeso C., D. Doser, J.E. Leyva, E. Rascon, F. Gómez and M. Domínguez A.

Introduction

Ciudad Juárez, Chihuahua is located in the central Chihuahuan Desert; with El Paso, Texas the cities form the twin Paso Del Norte metroplex (Figure 1a). This region of the Chihuahuan Desert is characterized by a semiarid climate with low precipitation rates (300 mm/yr) (Laboratorio de Climatología y Calidad del Aire-LCCA, 2008) occurring during the rainy season from early June to late August (LCCA, 2008). Summer rains in this area occur mainly in the form of heavy storms of short duration. Some of these storms can discharge large amounts of water within minutes to a few hours (Comisión Nacional del Agua CNA, 2008).

Hydrologically the region is divided into eight major basins (Instituto Municipal de Investigación y Planeación IMIP, 2004). The 2006 and 2008 floods were caused by intense rainstorms responsible for 30 to 50% of the total yearly precipitation in less than 24 hours (LCCA, 2008). The urban area of El Barreal was developed after 2003 for residential and commercial use (Buró Nacional Inmobilario BNI,
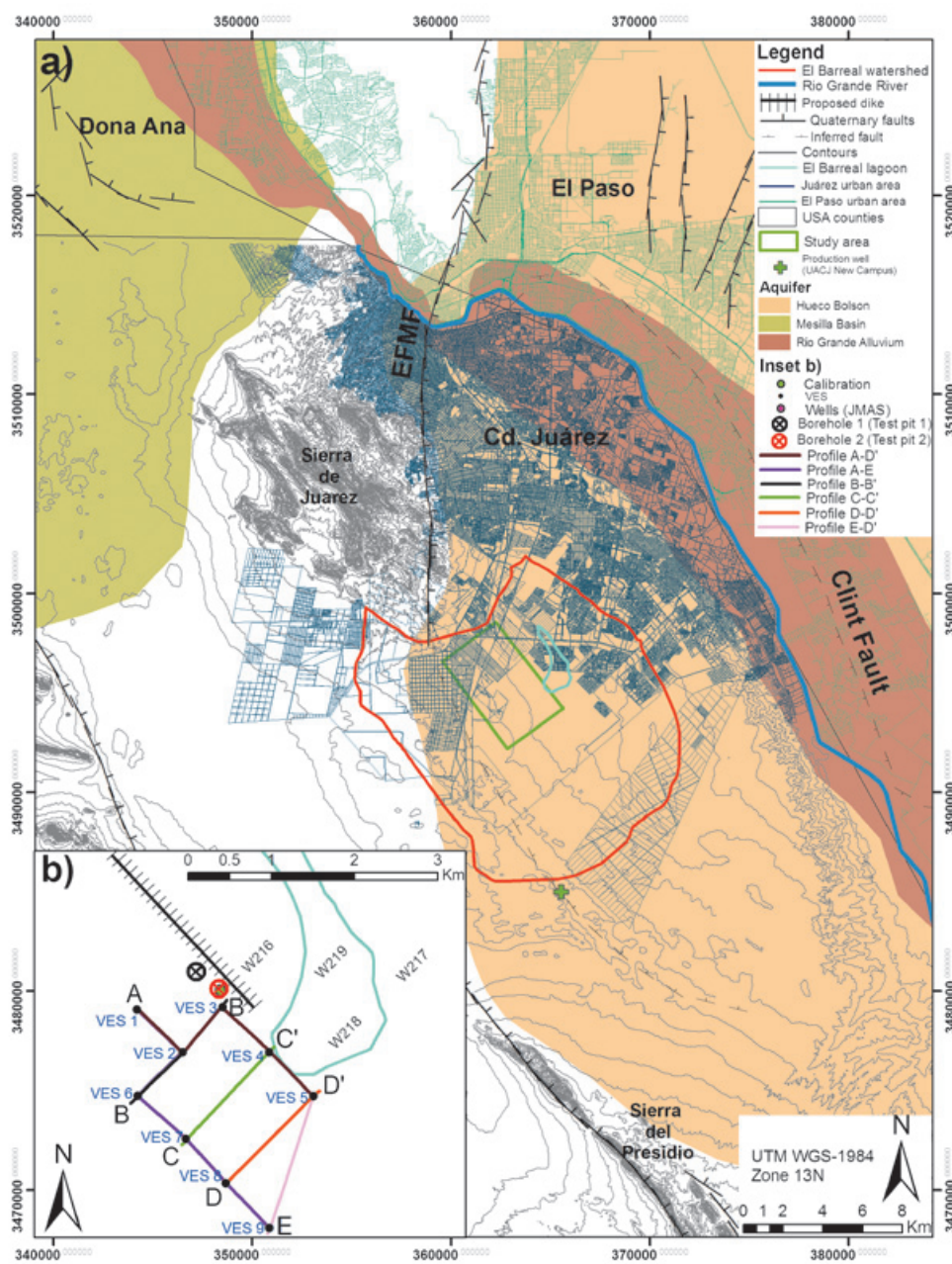

Figure 1. a) Regional location map. b) Inset of the study area (Green square). Letters represent geophysical profiles, the black hatched line represents the proposed dike and the pink dots represent the production well data available in the area. The trenches excavated to calibrate geophysics and perform open pit permeability tests are represented by black and red circles. Black dot represents location of Wenner array VES.

2009). Recommendations of the City Planning and Research Institute (IMIP) suggested preservation of the lake area, based on evidence from both hydrological modeling and historical records that it would flooded. Some small earth dams upstream (BNI, 2009) failed, chiefly due to lack of compaction and presence of impermeable clay cores, and a few absorption wells were unable to remove surface water as fast as it accumulated. During the July 2008 storms, the low lying area was totally flooded.

The State urban development offices (Secretaría de Desarrollo Urbano y Ecología, SEDUE) considered a solution consisting in a partial restoration of the lake area and the injection of excess water volumes into permeable strata of a shallow aquifer. A row of properly designed infiltration wells would be emplaced along a man-made embankment (Figure 1b).

Nine vertical electric soundings (VES) were performed with a Schlumberger array to delineate the depth and extent of non-permeable clay layers and the subsurface geometry of a sand body with enough permeability to store and deflect the excess runoff into the shallow aquifer. Two trenches were excavated to calibrate the geophysical findings and perform permeability tests of the selected strata. The geophysical survey proved to be an economical solution to image the depth and geometry of subsurface strata, which together with permeability results, led to a proper design for the injection of excess runoff during a major storm.

Background Studies

Hydrologic Setting

The Paso Del Norte region is located in the Basin and Range physiographic province. The topography of the Basin and Range is characterized by the presence of NNW trending mountain ranges and intermountain basins (Bolsons) with flat playa lakes (Hawley, 1993; Haenggi, 2002). Some playa lakes were formed as perennial pluvial lakes in late Pleistocene and especially during the last glacial maxima (early Wisconsin) (Hawley, 1993; Reeves, 1969). The largest Pleistocene Lake Palomas, covered an area inundating close to 7,800 km^2 in the bolson de Los Muertos (Reeves, 1969), approximately 60 kilometers southwest of the study area. These glacial lakes served as sinks for large hydrological basins often drained by two or more fluvial systems. The basin of El Barreal was not mentioned among the large glacial lakes (Reeves, 1969; Hawley, 1993; Allen, 2005; Castiglia and Fawcett, 2006), because of to its smaller area (only 164 km^2), and the absence of paleoclimatic studies.

El Barreal is a closed basin that drains the southeast Sierra de Juárez and adjacent highland areas (Figure 1a). The center of the basin is occupied by a flat playa covering an area of 2.3 km^2. There is 15 m of relief between the lowest point at the center of the basin and the highest point near Sierra de Juárez, and 3 m relief from the eastern boundary of the watershed to the center of the basin. Three to four midsize water streams (5-6 m crossections) discharge into the basin (Figure 2b). Sediments in the basin surface range from sand to silt and clay towards the center of the basin.

The watershed of El Barreal covers approximately 164.114 km^2 (IMIP, 2004b), yielding an approximate runoff of 1,318.37 m^3 (IMIP, 2004), for an average yearly precipitation of 300 mm (LCCA, 2008). This relatively large mass of water is transported by several first and second order intermittent streams that drain the runoff into a lower area defined by the 1,160 m elevation contour line, the historical boundary of the Laguna de Patos (El Barreal) (IMIP, 2004b). However, the flooded area could cover up to 6 km^2 unless hydraulic facilities are developed to contain the runoff (IMIP, 2004b).

The city granted permits for urban development, on the condition that earth dams were constructed upstream from the playa (IMIP, 2004b). However, this approach was not successful. In July 2008 the dams failed (Juárez Press, 2008).

Geologic Setting

The study area is geomorphologically defined as a flat, low-lying, desert playa flanked to the north by the Sierra de Juárez and to the south by Sierra del Presidio (Figure 2a). These mountain ranges and intervening basins represent the classic setting of the Basin and Range physiographic province, which is an uplifted region that records lithospheric thinning, extension and magmatism during the Tertiary (Keller and Baldridge, 1999). However, despite of the proximity to the Basin and Range province, the area of study actually lies within the southern portion of the Río Grande rift tectonic province as evidenced by a series of geological and geophysical features such as basin size and depth, presence of Quaternary tectonic activity, and crustal thinning (Seager and Morgan, 1979; Sinno *et al*., 1986; Keller *et al*., 1990; Averill, 2007), which differentiates the Río Grande rift from the Basin and Range (Keller and Baldridge, 1999).

As consequence of the tectonic setting, several main faults bounding the Hueco Bolson aquifer have been identified (Seager, 1980;
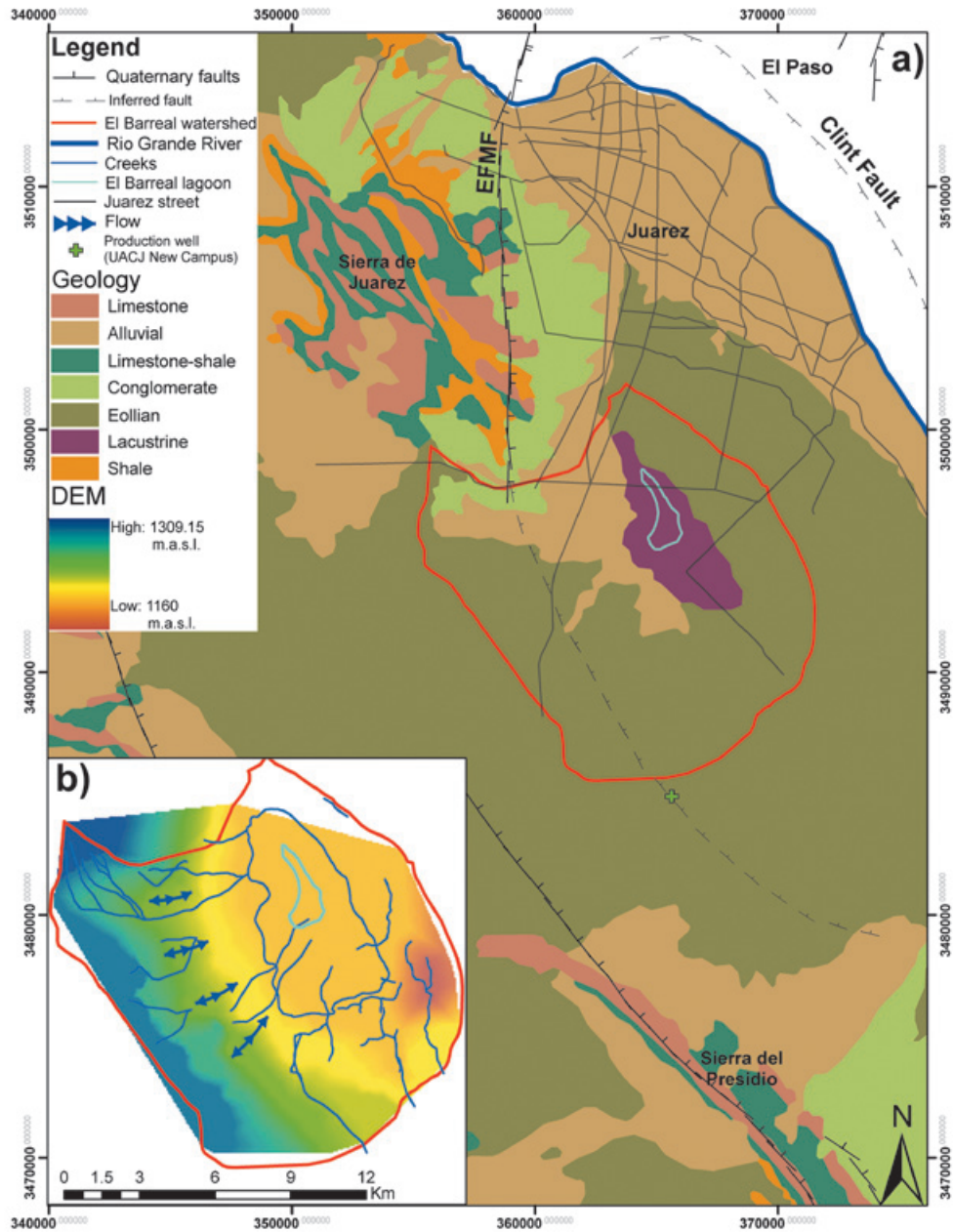
Figure 2. a) Geology of the El Barreal. Black hatched lines represent Quaternary faults and black spaced lines represent an important inferred fault by Burgos (2004) in the region. b) Inset of the El Barreal watershed showing flow patterns and the boundary (navy) of the ephemeral playa lake.

Burgos, 1993). Likewise intrabasin minor faulting, which has surface expressions, has also been reported (Sayre and Livingston, 1945; Knowles and Kennedy, 1956; Seager 1980; Burgos, 1993; McCalpin, 2006). The major faults flanking the basin are, at the western basin boundary, the East Franklin Mountain Fault (EFMF) and its prolongation into the Sierra de Juárez, and the Hueco Mountain fault that bounds the Hueco Bolson to the east (Figures 1 and 2a). The minor intrabasin faults scarps constitute an array of horsts, grabens and tilted

blocks in basin fill deposits (Seager, 1980). The other structural feature in the area is the Clint Fault, which is a major intrabasin fault inferred from analysis of stratigraphic data (Uphoff, 1978) that runs alongside the Río Grande marking the westernmost limit of the Diablo Platform uplift (Burgos, 1993). The age of the fault systems has been dated as 64.1 Ka by recent Infrared-Stimulated Luminescence Geochronology and sedimentology studies (McCalpin, 2006), which are half as old as the age assumed by Keaton and Barnes (1996).

In terms of sedimentation, the stratigraphic record of the area is comprised of varied depositional environments. The bedrock in the vicinity of the area is found approximately at 400 m depth (Burgos 1993; Rascón and Gómez, 2007; Dena, 2007; Obeso, 2008) and is commonly composed of carbonates from the Chihuahua Trough (Haengii, 2002). The sediments atop the basement represent a mixture of fluvial, lacustrine and terminal deltaic deposits derived from the ancient (post-Kansan) Río Grande deposits (Reeves, 1969) as it filled the structural basin formed by the Río Grande Rift, which through continued Neogene uplift again exposed part of the sediment package at the surface (Keller and Baldridge, 1999). The sedimentary depositional environment of the deposits is commonly referred to as "alluvial" (Kernodle, 1992), in spite of the significant amounts of fluvial, lacustrine, and aeolian sediments that form these complex landforms (Hawley 1969; Hawley *et al*., 2000; Hawley *et al*., 2001). Modern surficial deposits atop the basin include a varied series of sedimentary environments, resembling at smaller and localized scales the ancient fluvial Río Grande and terminal (alluvial-lacustrine) depositional systems. These deposits, especially near the Sierra de Juárez, commonly accumulate in small endorheic micro-basins (e.g., study area) and are characterized by a series of fluvial (stream) and alluvial (fan) deposits found in the upstream (piedmont) areas of the basin. Terminal fan deposits and their associated feeding streams are found at the upstream margins of the playa lakes commonly located in the center or lowest elevation areas of the basins (Figure 2a). The central areas of the basins are dominated by fine grain size sediments accumulating in thick (several meters) layers intercalated by lenses or thin layers of coarser sand size deposits, as found in the production well data (Figure 3) from wells located close to the area of study (Figure 1b) provided by the Juárez Water Utility office (JMAS). These layered sediments would have been deposited by the progression of a terminal fans feeding streams on to the playa areas and their subsequent abandonment and covering by the continuing deposition of lacustrine deposits. Surficial playa deposits in the study area are surrounded by a thin and non-extensive aeolian sand sheet and overlaying nebkha dunes.

Geophysics

The shallow stratigraphy of El Barreal has not been formally described and there are no published geophysical studies that would aid in the location and visualization of any permeable strata geometry. Only isolated technical reports related to the construction of absorption wells exist, but are not available to the public.

Several previous geophysical studies have examined both the regional tectonic and stratigraphic setting chiefly in the Hueco Bolson; Keller and Baldridge (1999) summarized the geophysical work done in the area that resulted in the geographic distinction, in terms of tectonic provinces, between the Basin and Range and Río Grande Rift as well as an explanation of the rift evolution. More recently, Averill (2007) conducted Wide Angle Reflection and Refraction (WARR) studies that revealed the lithospheric structure beneath the rift, as well as the basin architecture. On a more local scale, O'Donnell (1998) conducted seismic reflection studies that mapped the basement at depths of 400 meters. Gravity studies have also revealed the presence of regional faults (Burgos, 1993), and the presence of Quaternary faults (Khatun *et al*., 2007) and fracture zones suitable to be infiltrated by brines into the aquifer (Granillo, 2004). On the Mexican side of the border, an undulating bedrock surface formed by a series of horst and grabens at depths greater than 400 meters has been also modeled from gravity studies (Dena, 2007; Obeso, 2008). In the case of magnetic data, the Ciudad Juárez aeromagnetic chart (Servicio Geológico Mexicano (SGM), 2008) reveals the presence of intrusive bodies in the vicinity of the Sierra de Juárez, but the magnetic field intensity is relatively low in the El Barreal area. Time Domain Electromagnetic (TDEM) soundings (Rascón and Gómez, 2007) have mapped the basement at depths of 400 meters in strong agreement with the gravity studies conducted in the same area (e.g., Dena, 2007; Obeso, 2008). The textural discrimination of the sediment package was also inferred from TDEM studies, since it is widely documented (e.g., Telford *et al*., 1995; Sharma, 1997; Palacky, 1987; Dena, 2000; Doser *et al*., 2004) that clay dominated textures show lower electrical resistivity and magnetic susceptibility values than sand units. Rascón and Gómez (2007) also correlated the final results of TDEM studies and electrical resistivity logs with the lithology (Figure 4) of an exploration well drilled approximately 10 km south of the southern tip of El Barreal (Figure 1a). Their results showed that low resistivities were indeed associated with fine grain textures. The relatively low resistivity observed at depths ranging between 75 and 200 m was due to the presence of moderately good quality groundwater (Figure 4). This unexpected effect, could be the consequence that in a relatively clay dominated sedimentary units, the low resistivity might be attributed to the clay itself exclusively, and not necessarily to low quality water, as can be concluded from theoretical petrophysical calculations (Shevnin *et al*., 2003). Nevertheless none of these geophysical studies were conducted specifically at El Barreal, and none of them had the specific goal of discriminating the shallow stratigraphy in the detailed fashion required in this study.
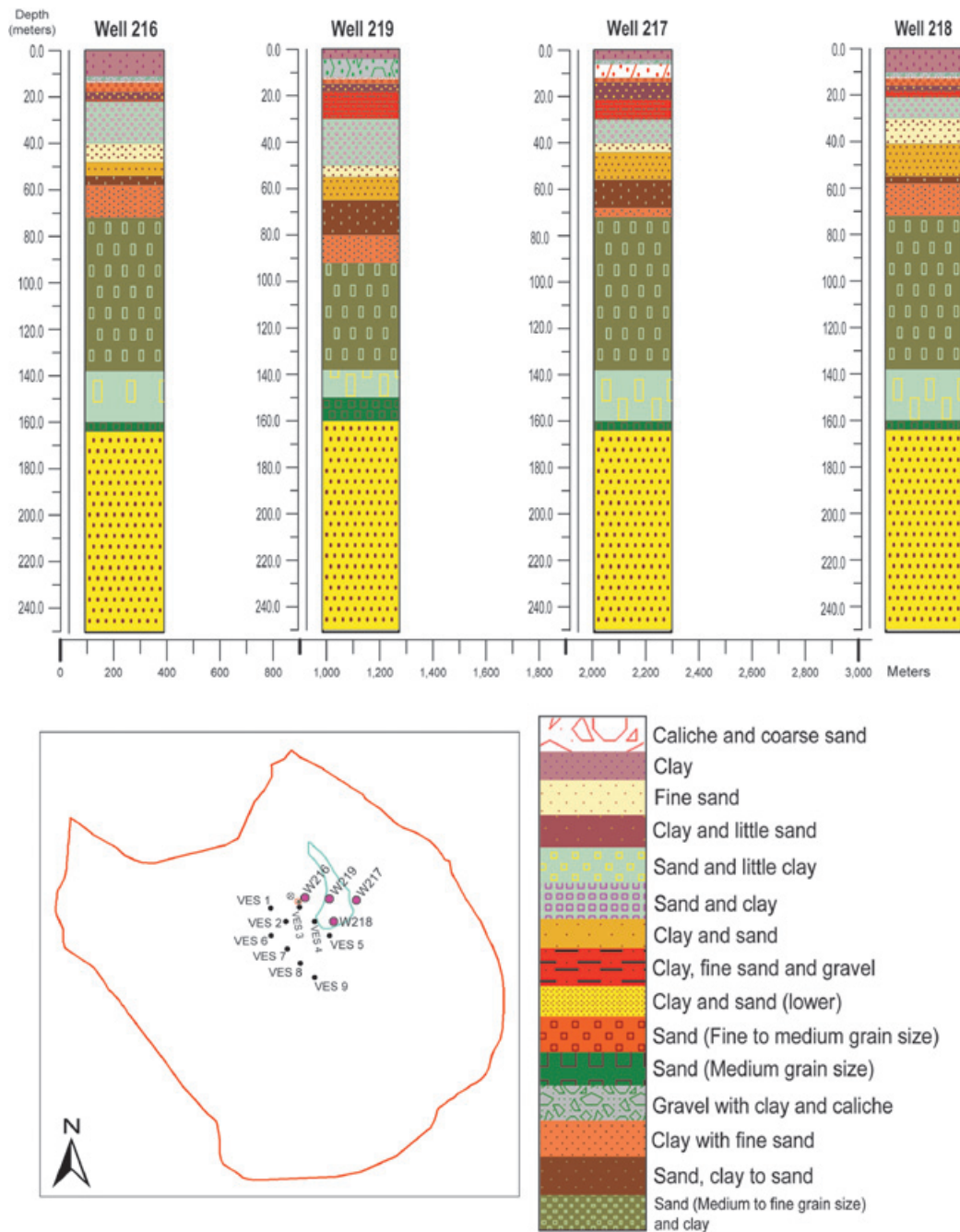
Figure 3. Production well lithology data.

Methodology

The methodological approach consisted of conducting an array sensitivity test to determine the best DC acquisition geometry to be deployed during the survey. The actual data acquisition was conducted utilizing the Schlumberger electrode array since it was shown to be sensitive enough to discriminate between sand and clay strata, and at the same time be the least time and crew intensive. As a result, a total of 9 Vertical Electrical Soundings (VES), with depths of penetration not deeper than the water table (~100 m) were acquired in the vicinity of the proposed dike (Figure 1b).
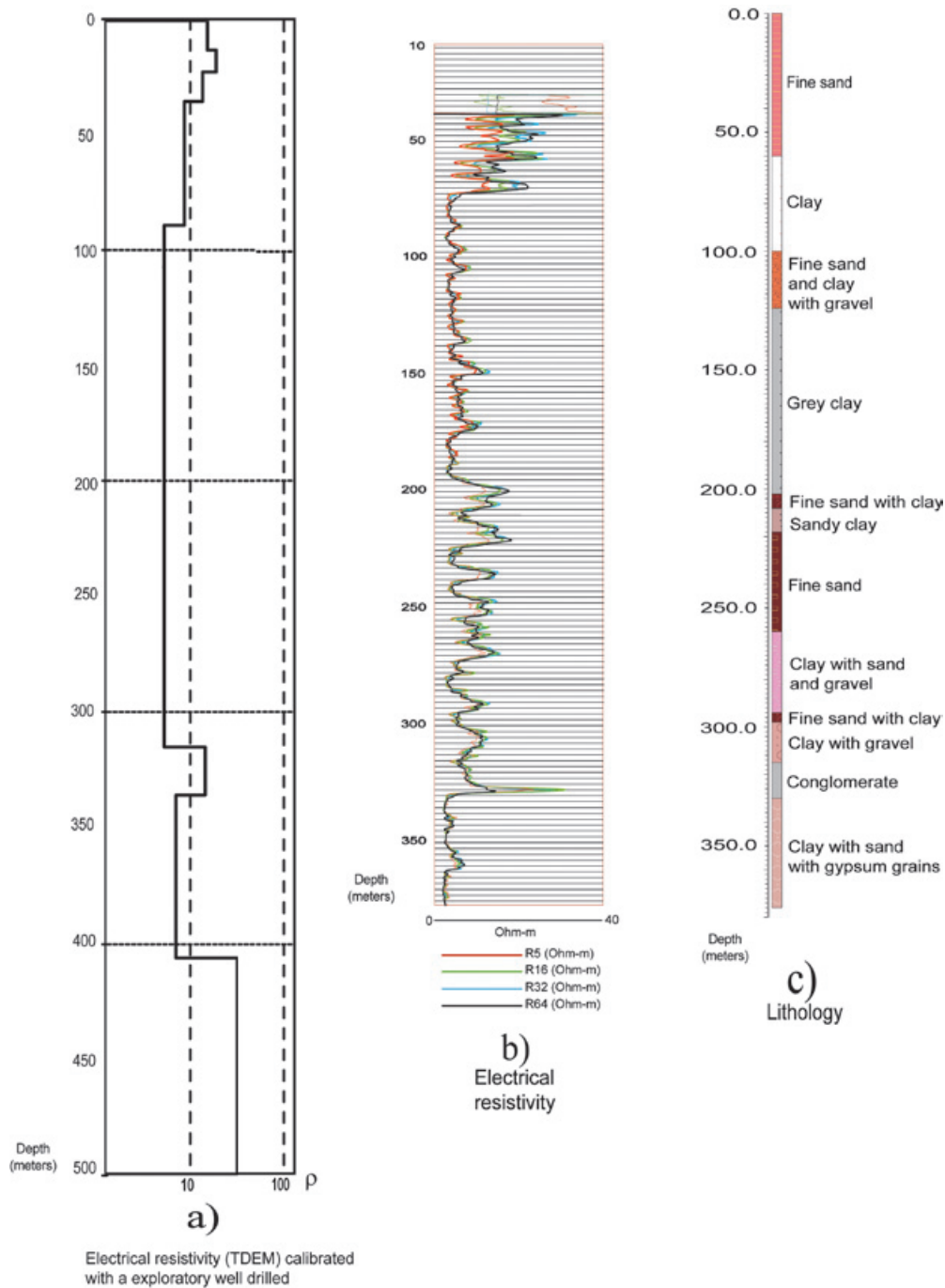
Figure 4. Geophysical and exploratory well studies in the vicinity of El Barreal watershed. a) TDEM 1D model. b) Electrical Resistivity log. c) Exploration well lithology data.

The initial resistivity curves were forward modeled with the software package IPI2win (Shevnin and Modin, 2003) to generate a preliminary geophysical model and to determine the locations of calibration trenches required to validate the geophysical findings. At one of the excavated trenches (borehole 2, Figure 1b) two extra VES using Wenner arrays, since they are more sensitive to vertical variations at deeper measurements than the Schlumberger electrode configuration (Loke, 2004), were recorded perpendicular to each other in order to test for resistivity anisotropy.

We next used the lithostratigraphic information from borehole number 2 to fix the first 14 meters of the models to known strata thicknesses, and the water table depth (known from the production water wells) was kept also fixed during the inversion process (also carried out with IPI2win), allowing the software to invert exclusively for resistivity using these geologic constraints. For the intermediate layers located at depths between 14 m and ca. 100 m we inverted for both resistivity and thickness. The calibrated 1D geophysical models were correlated to each other by gridding the inverted results using the linear triangulation method. Further post-processing and final graphics for the geophysical model were produced with the software package GMT (Wessel and Smith, 1988). The geological model was produced by assigning stratigraphic horizons to the resistivity layers obtained from inversion of the DC soundings using the software package Rockworks (Rockware, Inc.; 2002). The permeability was determined by pouring water into an open pit and applying a Lefranc variable flow test with the descending hydraulic head method conducted through an open pipe resting on the clean sand layer at the location of borehole 1 (Figure 1b). The subsurface strata infiltration capacity was estimated applying the constant head method. Finally, the study area was zoned in terms of subsurface hydrostratigraphic properties by integrating all the geophysical findings and geomorphologic analysis of satellite imagery into a geographic information system (GIS).

Data and modeling

Resistivity

Resistivity readings were collected with a TERRAMETER SAS 300C instrument (ABEM, 1993) and digitized on a field computer to visualize and determine if the observed slope changes in the apparent resistivity curves were reasonable or if the reading had to be repeated. To generate 1D models relating true resistivity to depth, forward modeling was carried out utilizing the available lithology in the groundwater exploration well database (Figure 3) as starting models. The final 1D model for each sounding was calibrated and inverted constraining the inversion with the lithology observed in the trench of borehole 2 and the water table depth of ca. 100 m as reported by the JMAS (Rascón, 2008). The final 1D inverted models, with RMS fits less than 5%, were correlated by using the triangulation method of linear interpolation between the layered models.

Permeability test

With the data collected in the field-time (min), and depth (m), we calculated each of the required variables to obtain the average permeability as follows: for each time interval (5 minutes) we determined the change in hydraulic head, and since the shape coefficient and the cross section of the shape are constant, we calculated the permeability for each time interval. After 81 minutes, the water had completely infiltrated into the ground, so we averaged the interval permeability. Once the average permeability was determined, the subsurface strata infiltration capacity was estimated (constant head method) with the following parameters: a 6 m length filtrant gallery, pipelines with inner ring casing diameters of 8, 12, and 16" (20.3, 30.5, 40.6 cm), and a maximum depth of 85 meters. The phreatic level is expected to be found at ca. 100 m and we assumed that it was not unlikely to find a sand dominated strata between depths of 12 m and 85 m since the lithology (Figure 3), and resistivity and gamma logs in nearby production wells supported our hypothesis of finding sand packages with similar grain size (Rascón, 2008).

Results

Apparent resistivity

The apparent resistivity curves (Figure 5) show how the sampled grain size related parameters vary geospatially, reflecting the presence of different resistivity families or domains in terms of the overall shape of the apparent resistivity curves. VES's 1, 5, 6, 7, 8 and 9 show "H" type curves indicating the presence of an anomalous low resistivity bed at intermediate depths (Telford et al., 1995). On the other hand, VES's 2, 3 and 4 show "A" type resistivity patterns that monotonously increase with depth.

Forward modeling

The initial results of the forward modeling (Figure 6a) of VES 3 and VES 4 showed that an interpreted clay layer could be overlaying a possible permeable sand body located at a depth of ca. 14 m. To confirm or reject these results, a trench was excavated at a distance of approximately 20 m NW of the VES 3 location. The observed stratigraphic units (Figure 6b) showed the presence of a coarse sand unit at a depth of 12 m, but a fine grain sand layer embedded in the clay layers was also observed between depths of 1.70 m and 7 m. Additionally, as mentioned earlier, two more VES were conducted next to the trench to detect if any anisotropy was present (Figure 7). Since no significant changes were observed between the soundings, we concluded that, at least with the resolution provided by our electrode array and instrument, homogeneity and isotropy was indicated.
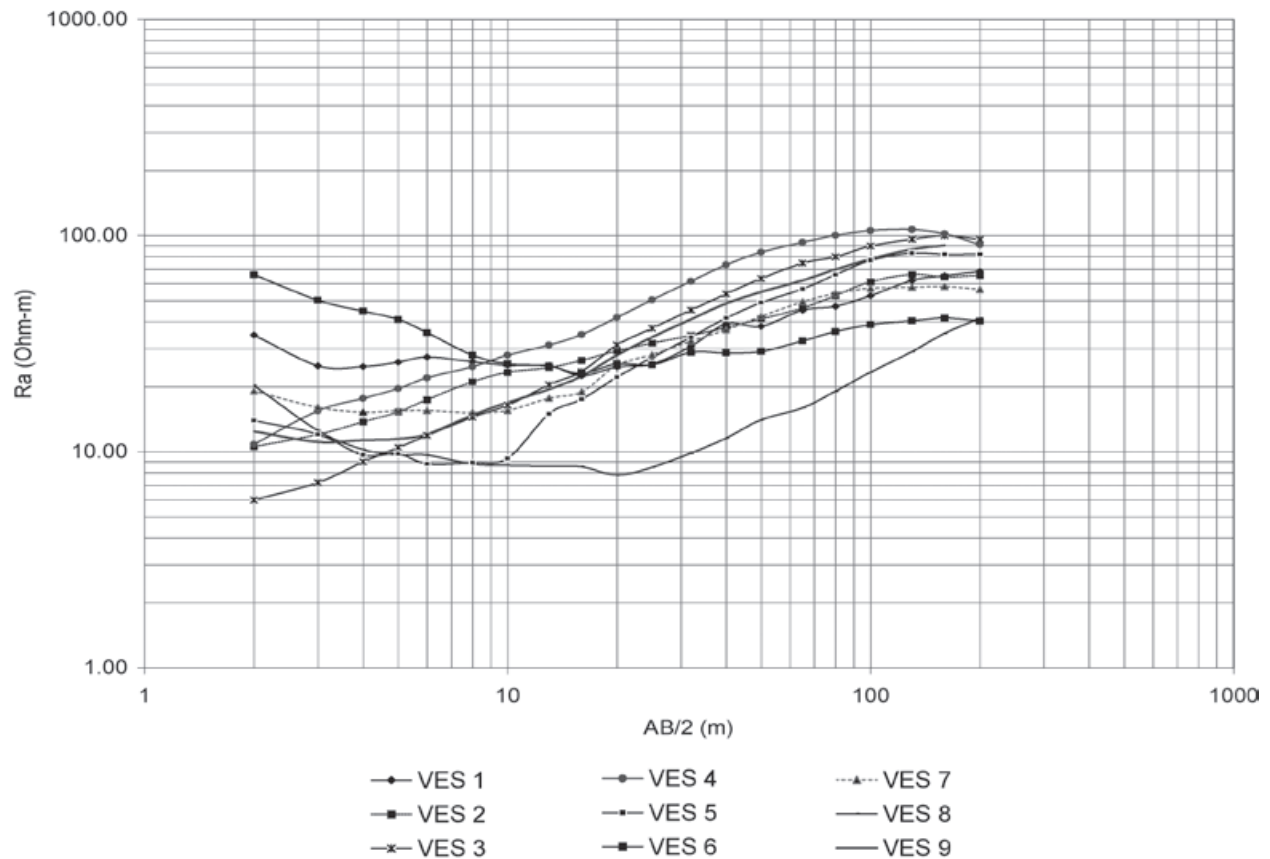
Figure 5. Apparent resistivity curves of the nine VES (Vertical Electrical Soundings) acquired at El Barreal utilizing the Schlumberger array. For sounding location see Figure 1(b).

Borehole tests

Two trenches were excavated (Figure 1b) to corroborate and calibrate the geophysical findings. The observed lithologic columns (Figure 8) are composed of 11 meters of lacustrine deposits at borehole 1 (BH1) (Figure 8a), and 12 meters of lacustrine deposits at borehole 2 (BH2) (Figure 8b). Within this sedimentary sequence, a package of fine sand with clay is found. The thickness of this layer is 5.5 m at BH2 and 9 m at BH1. The bottom of the lacustrine sequence at BH2 is composed of plastic clays and poorly compacted fine sands. These strata are not found at BH1, suggesting that during deposition a strong elevation gradient existed between the boreholes geographic locations because the flooding event is not recorded in both lithologic columns. Finally, a package of sediments with a grain size corresponding to fine to medium sands with no observed clays underlies the lacustrine sequence.

Inverted models

The most remarkable results obtained from the trench-calibrated final 1D inverted models (Figures 9, 10 and 11) are the presence of horizontal variations of the geoelectrical signature, expressed as the logarithm of the inverted resistivity, in the 2D models (Figures 12 and 13).

Based on these results several geoelectric units (G.E.U.) were defined by using ranges of resistivity values documented in global studies (e.g., Palacky, 1987; Sharma, 1997), local surveys (Dena 2007; Obeso, 2008; Rascón and Gómez, 2007), and the trench-calibrated resistivity responses of this survey. The classification resulted in six G.E.U.'s (Table I). The shallower units were correlated with the lithological column observed in the trench. The first unit (r < 15 ohm-m) is correlated with a clay dominated layer. The second unit (15 <r <
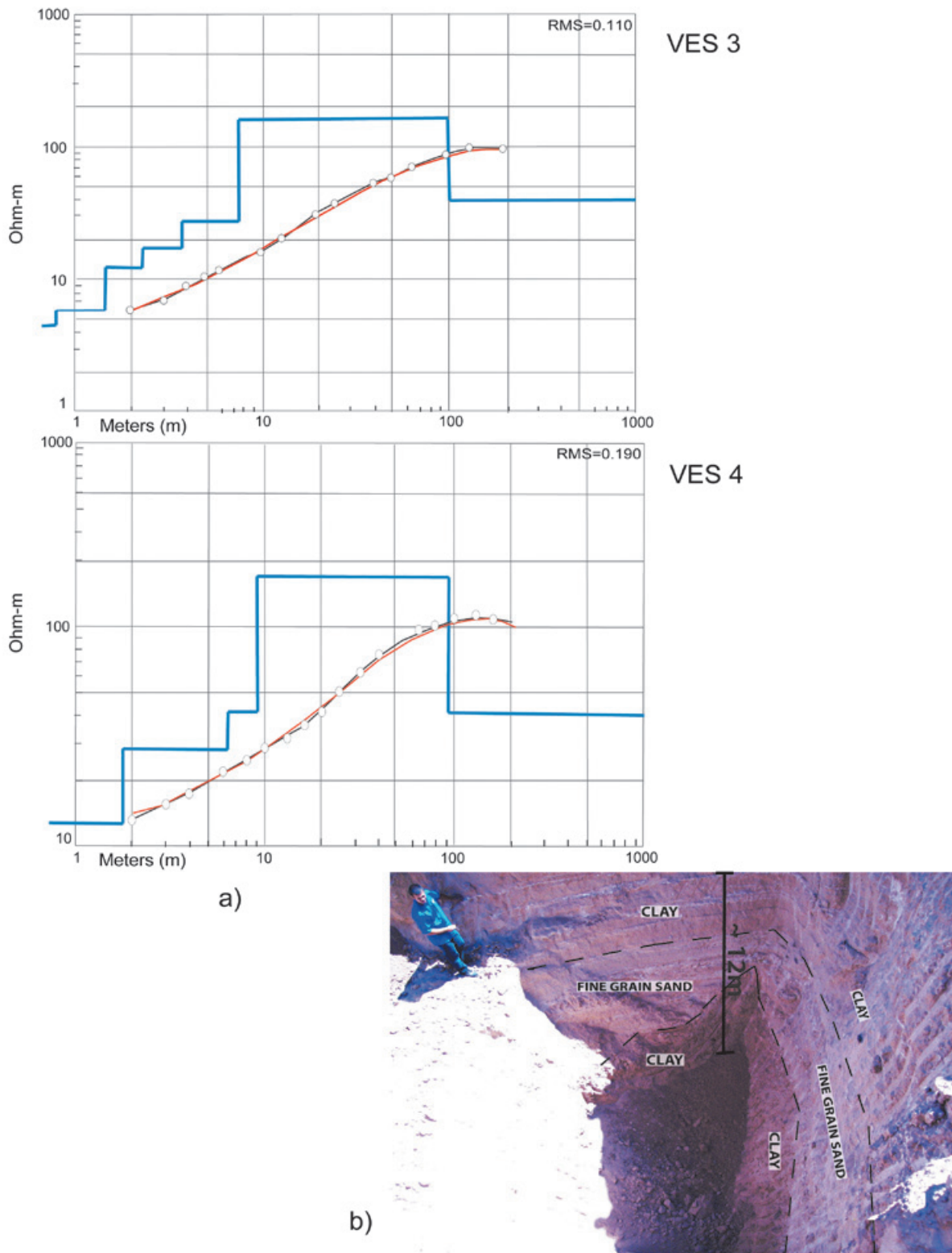
Figure 6. a) Initial forward modeling results. The observed points are represent by white dots, black line represents the resistivity curve of the observed points, red line represents the resistivity curve that best fits to the observed data curve, and the layers model is shown in blue line. b) Photograph of the excavated trench (Test pit) number 2.
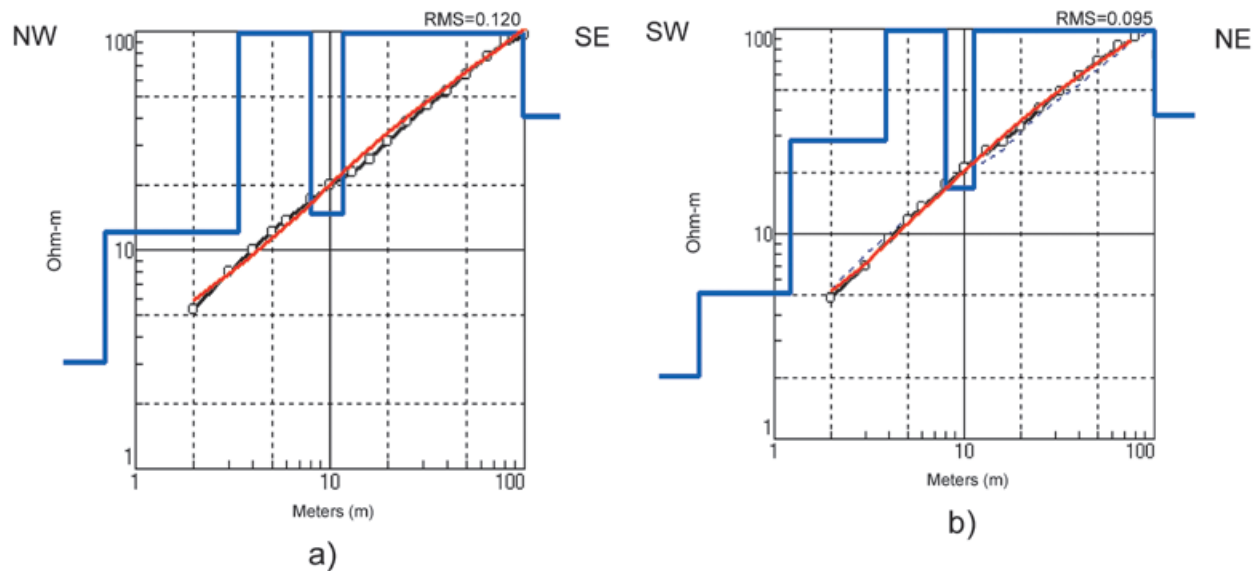
Figure 7. Wenner array VES conducted perpendicular to each other to test for anisotropy in the upper 30 m of depth. The observed points are represent by white dots, black line represents the resistivity curve of the observed points, red line represents the resistivity curve that best fits to the observed data curve, and the layers model is shown in blue line. For location see Figure 1(b).

50 ohm-m) is correlated with a fine grain sand layer, G.E.U. 3 (50 <r < 80 ohm-m) is correlated to compacted and cemented fine grain sands according to textural analysis. The deeper units were interpreted in terms of production wells since the excavated trenches did not reach depths greater than 14 m. G.E.U. 4 (80 <r < 160 ohm-m) is associated with the presence of medium grain sands with some clay. G.E.U. 5 (160 <r < 270 ohm-m) is interpreted as a thick package of non-cemented fine to medium grain sand. Finally, G.E.U. 6 (30 <r < 70 ohm-m) is associated with the top boundary of the aquifer, which, according to well data, is composed of medium to coarse grain sands.

Permeability

The permeability was calculated for each time interval with the data collected in the field. The resultant average permeability (2.48 m/d) was determined from 6 interval permeabilities (Table II).

The permeability test (Figure 14a) shows how the infiltration rate depends on the hydraulic head, i.e., the higher the charge, the faster the infiltration. Furthermore, this analysis reveals that permeable layers are found at depths close to the infiltration test depth. The estimated infiltration capacity results (Figure 14 b) display the projected infiltration yields for each inner ring casing diameter considered.

Table 1. Geoelectric Units (G.E.U.).

Unit	Lithology	ρ (Ohm-m) resistivity
G.E.U. 1	Clay (plastic)*	< 15
G.E.U. 2	Fine grain sand with clay*	15 - 50
G.E.U. 3	Fine grain sand compacted and cemented*	50 - 80
G.E.U. 4	Medium grain sand with some clay **	80-160
G.E.U. 5	Fine grain clean sand, not cemented **	160-270
G.E.U. 6	Aquifer (Medium to coarse grain sand)**	30 – 70

Source: *Test Trench, ** Production wells, JMAS.

Table 2. Open pit permeability test results.

Time (min)	Depth to the level (m)	H0-H1 (m)	t0-t1 (min)	C (1/m)	A (m2)	k (m/min)	k (m/d)
8	0.160	0.600	8	1.5665	0.03243	0.001499	2.16
18	0.340	0.420	10	1.5665	0.03243	0.001672	2.41
28	0.444	0.316	10	1.5665	0.03243	0.001590	2.29
39	0.551	0.209	11	1.5665	0.03243	0.001680	2.42
49	0.620	0.140	10	1.5665	0.03243	0.001752	2.52
66	0.712	0.048	17	1.5665	0.03243	0.002124	3.06
81	0.760	0.000	15	1.5665	0.03243		
						Average	**2.48**
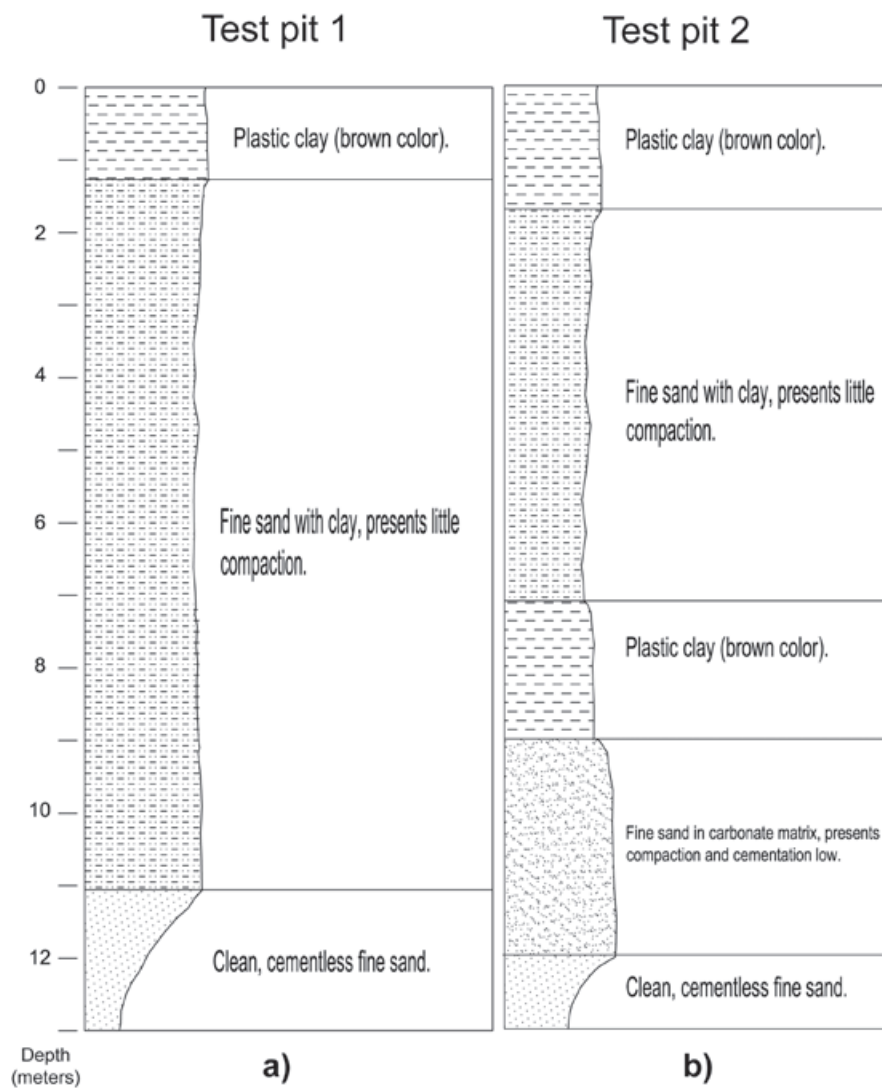
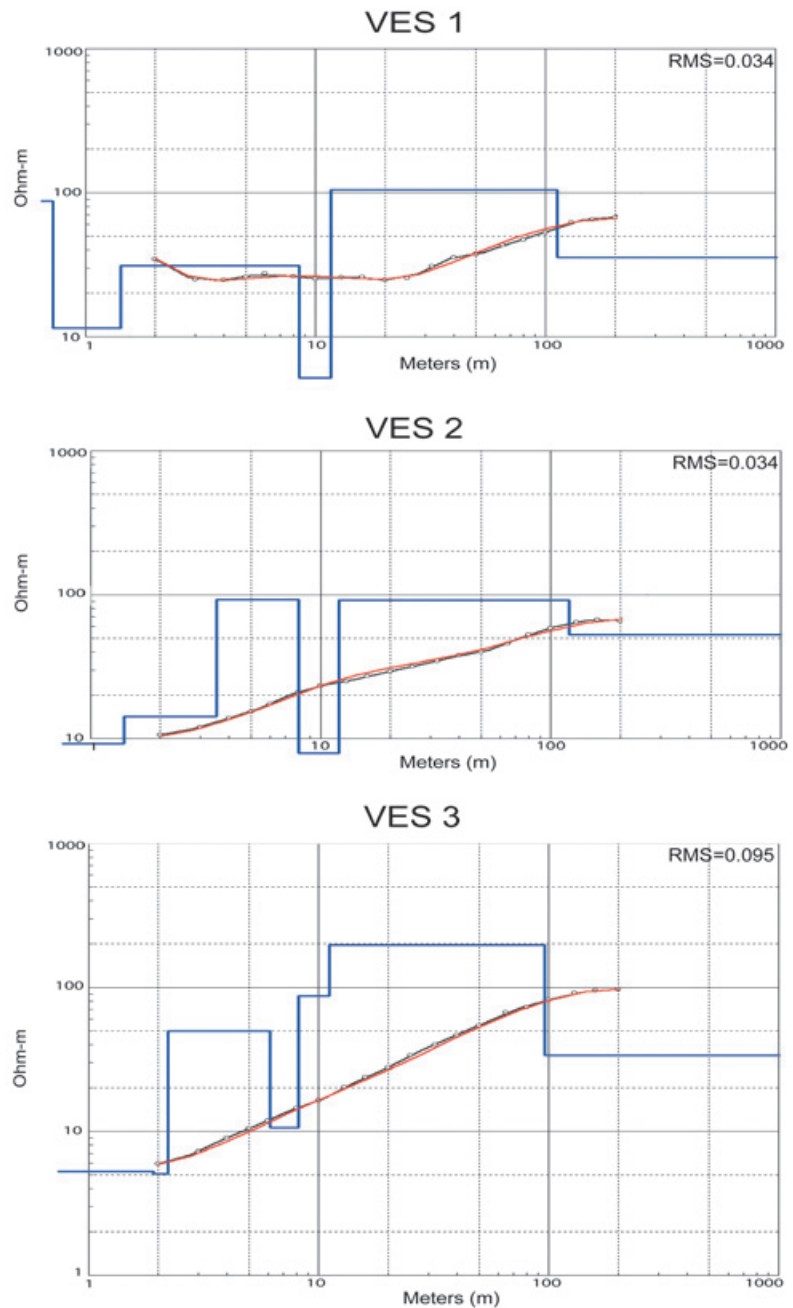**Figure 8.** Excavated trench lithologies.

Figure 9. VES 1, VES 2, and VES 3 1D inverted models. The observed points are represent by white dots, black line represents the resistivity curve of the observed points, red line represents the resistivity curve that best fits to the observed data curve, and the layers model is shown in blue line.

Discussion

The application of DC Electrical methods at the El Barreal flooding zone reveals six different G.E.U. (Figures 12 and 13), which were associated with specific lithologies (Table I) identified either in the excavated trenches (Figure 8) or the production wells (Figure 3). The interpretation of these G.E.U., together with the correlation between the 1D inverted models (Figures 9, 10 and 11), revealed the subsurface geometry of the stratigraphic package within the study area. The final stratigraphic sections (Figures 15 and 16) show how the interpreted lithofacies in profiles A-D', B-B', C-C' and B-E' reveal lateral heterogeneity associated with the strong lateral gradients observed in the geophysical profiles between VES1, VES2, VES3, VES4 and VES5 (Figure 12a), VES6, VES2 and VES3 (Figure 12b), VES7 and VES4 (Figure 12c), and between VES6, VES 7, VES8 and VES9 (Figure 13c). On the other hand, stratigraphic sections D-D' and E-D' (Figure 16a and b) appear more homogenous as suggested by geophysical profiles between VES 8 and VES 5 (Figure 13a) and VES9 and VES5 (Figure 13b).
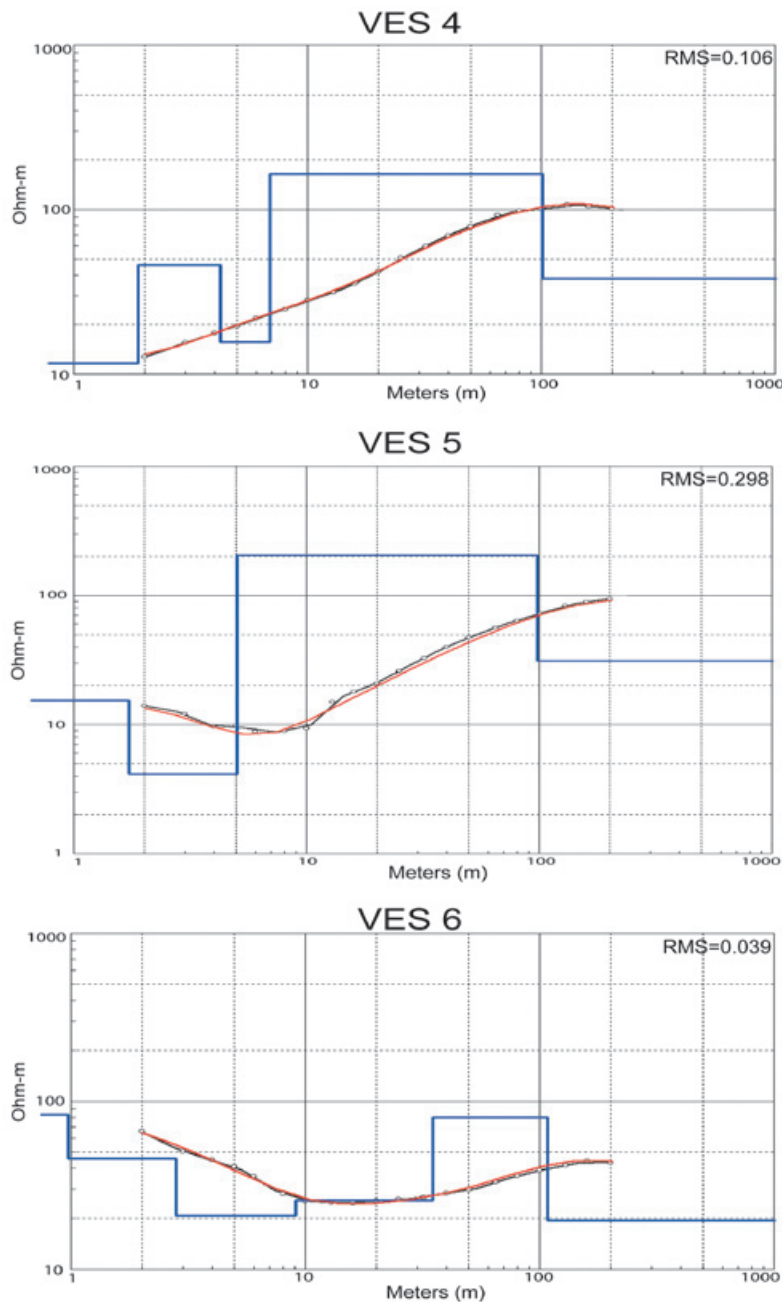
VES 4

VES 5

VES 6

Figure 10. VES 4, VES 5, and VES 6 1D inverted models. The observed points are represent by white dots, black line represents the resistivity curve of the observed points, red line represents the resistivity curve that best fits to the observed data curve, and the layers model is shown in blue line.

The lateral transitions in sections A-D', B-B', C-C' and B-E' are associated with the presence of larger grain sands pinching out into a layer composed of sand and clay. This lateral heterogeneity is more evident in the 3D model of the investigated area (Figure 17). The geometry of the relatively coarse and permeable sand seems to be consistent with the architecture of deposition of prograding deltas and terminal fan deposits developed by ephemeral streams. The strong geophysical gradients might be interpreted as the boundary of a series of paleochannels or ancient prograding deltas, probably developed as a consequence different flooding events. This interpretation seems to be consistent with the

geomorphologic features observed in the satellite image of the El Barreal watershed (Figure 18).

As an alternate explanation, the observed heterogeneity patterns could also be explained in terms of the presence of Quaternary faults that are common in the region (Seager, 1980; Burgos, 1993; Khatun *et al*., 2007; McCalpin, 2006). The inferred EFMF, which is 500 Ka old (McCalpin, 2006), passes very close to the area of study (Figures 1a and 2a). Furthermore, it is very possible that the pattern of faulting observed in the northwestern Hueco Bolson (e.g., Seager , 1980), consisting of a series of intrabasin horsts and grabens is also taking place in the El Barreal
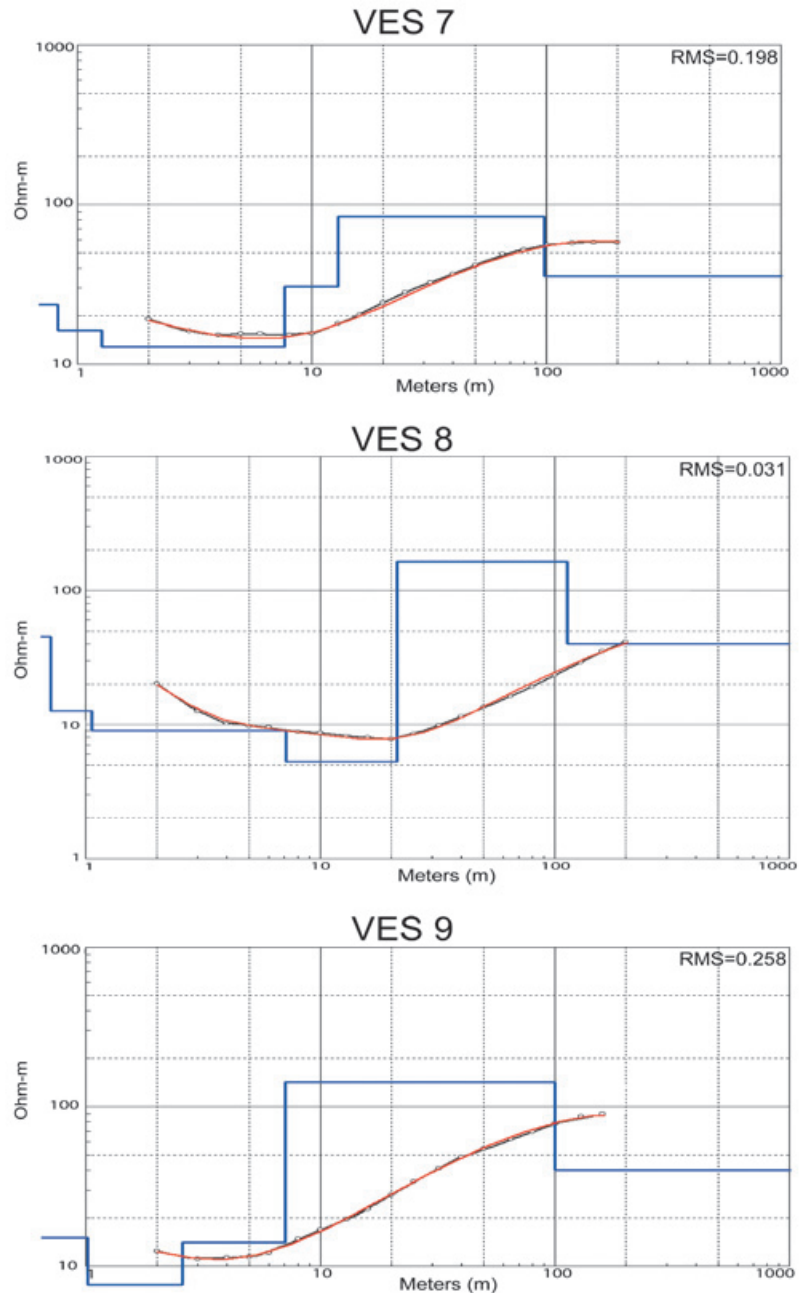
VES 7

RMS=0.198

Ohm-m

Meters (m)

VES 8

RMS=0.031

Ohm-m

Meters (m)

VES 9

RMS=0.258

Ohm-m

Meters (m)

Figure 11. VES 7, VES 8, and VES 9 1D inverted models. The observed points are represent by white dots, black line represents the resistivity curve of the observed points, red line represents the resistivity curve that best fits to the observed data curve, and the layers model is shown in blue line.

zone located within the southwestern Hueco Bolson (Figure 1a), within the Río Grande Rift. The fact that fault scarps are not observed at the surface in the study area could be attributed to recent alluvial processes that have covered them. Other geophysical techniques, such as precision gravity surveys, could help reveal how extensive faulting is within this region.

Regardless of whether the deposition patterns are either attributed to structural or stratigraphic controls or both, a final hydrostratigraphic zoning (Figure 18), useful for the immediate purpose of infiltrating runoff excess into the shallow aquifer,

was developed by integrating the geophysics and permeability results, production well data and geomorphology, into a geographic information system. As a result, two hydrostratgraphic zones are proposed: (I) The area located southeast of VES 3 (green polygon in Figure 18) seems to be the most suitable region to be successfully infiltrated by runoff in terms of the geophysical and direct test findings, and (II) the red polygon (Figure 18), which on the other hand, seems to be overlying a low permeability clay-prone zone, which lacks the potential to effectively support the infiltration well battery design.
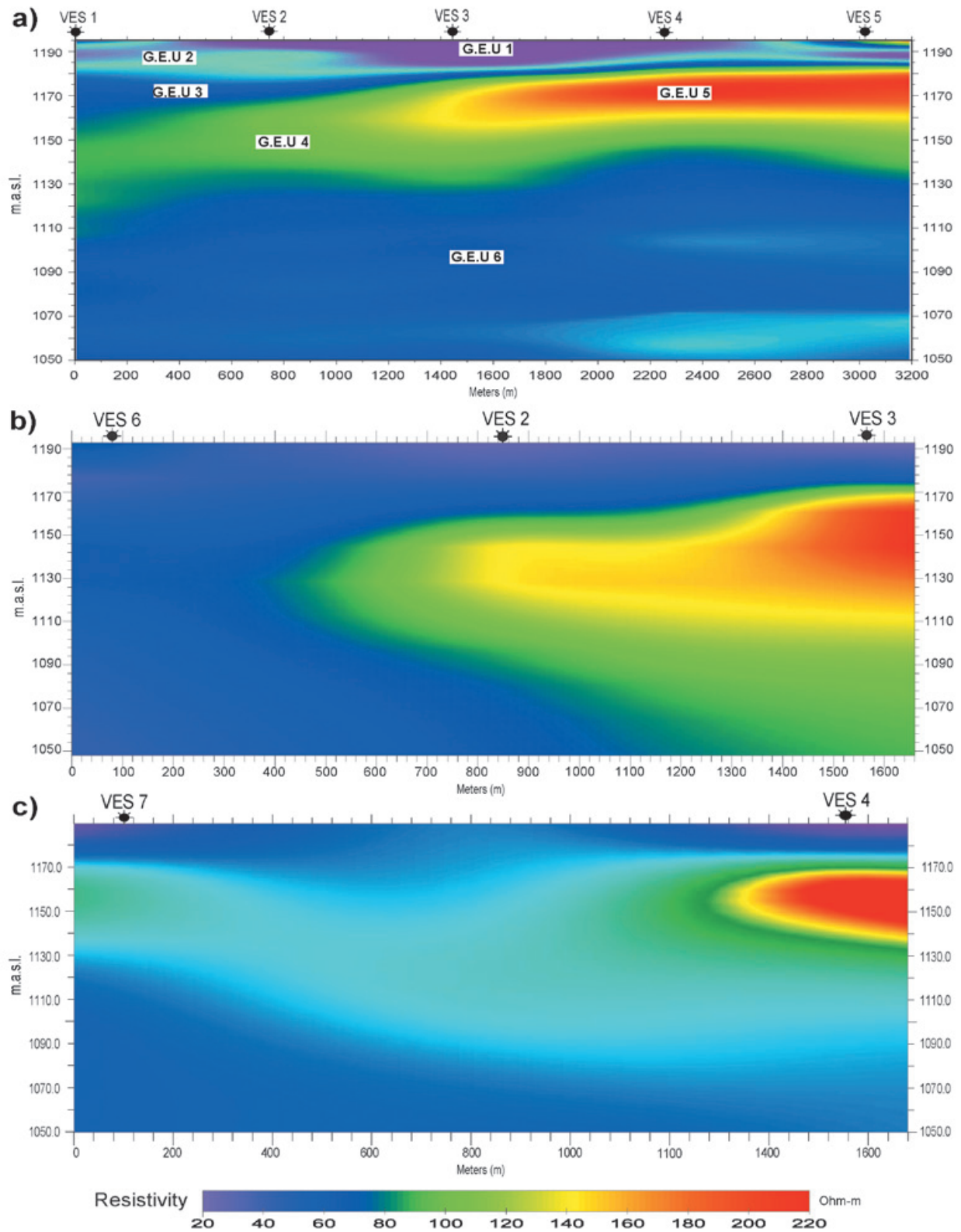
Figure 12. Geoelectric 2D models generated by interpolation between the 1D inverted models. For location see Figure 1(b). Resistivities are represented as the logarithm of the inverted resistivity.
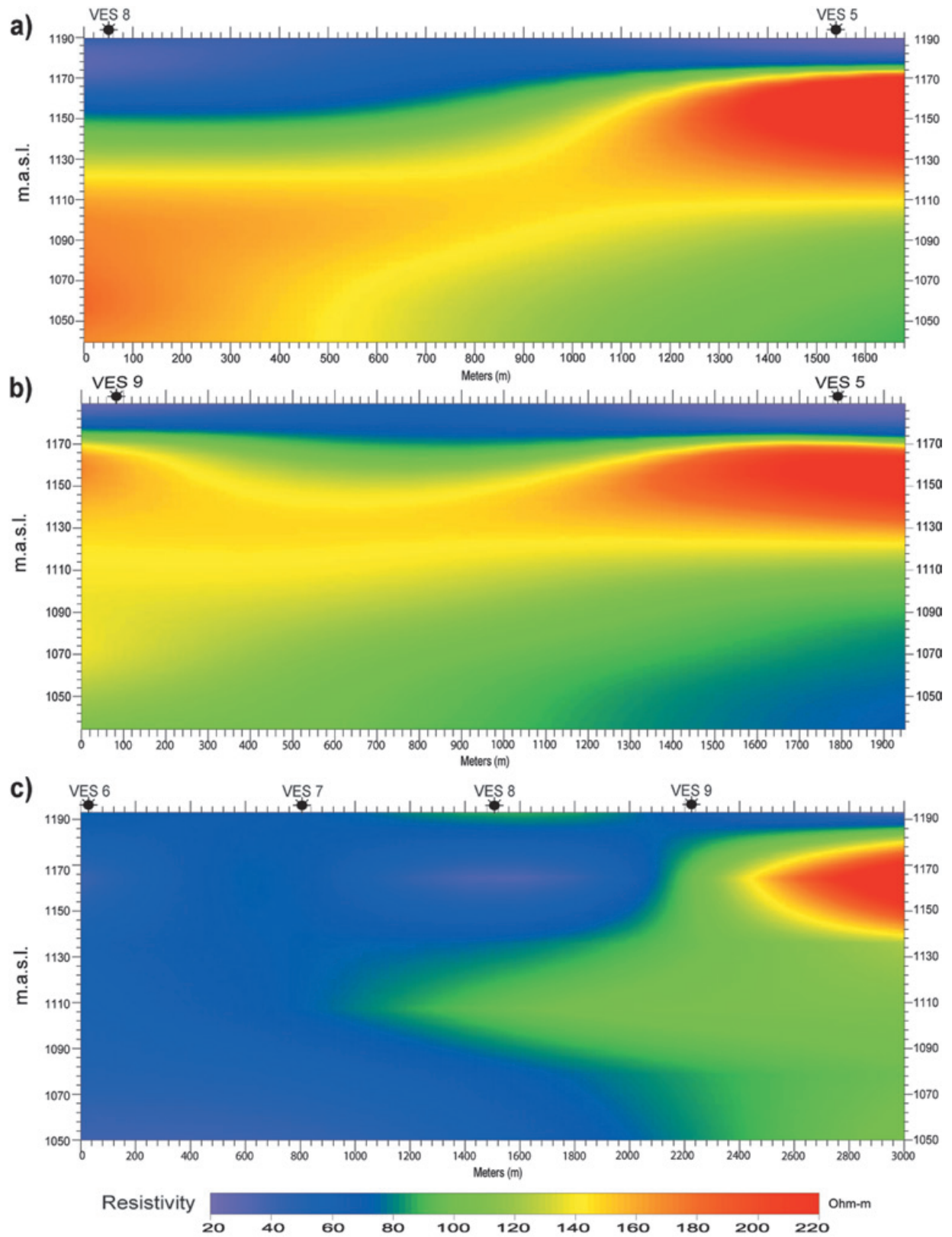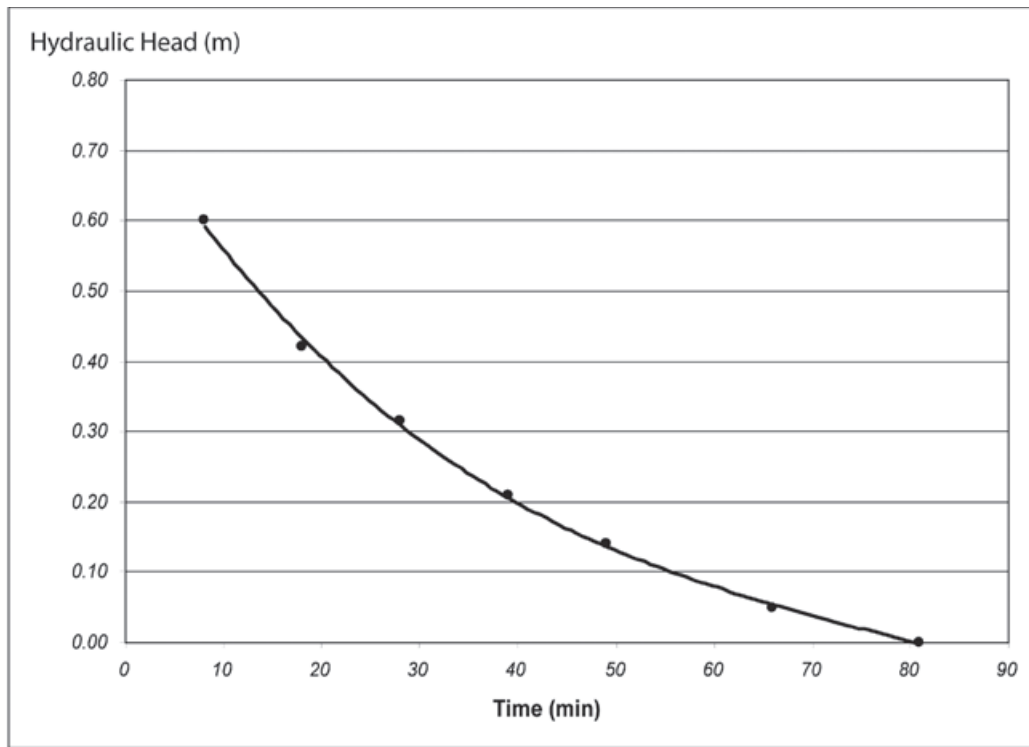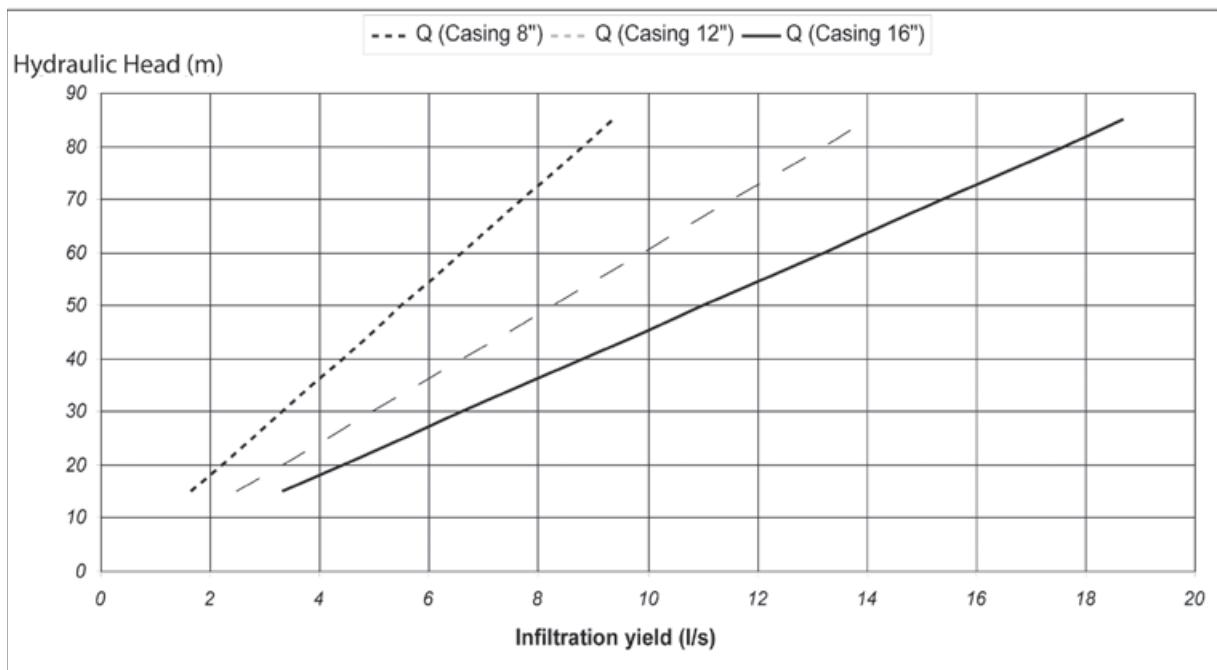
Figure 13. Geoelectric 2D models generated by interpolation between the 1D inverted models. For location see Figure 1(b). Resistivities are represented as the logarithm of the inverted resistivity.

a)

b)

Figure 14. a)Lefranc permeability test pit results. b) Infiltration capacity results.
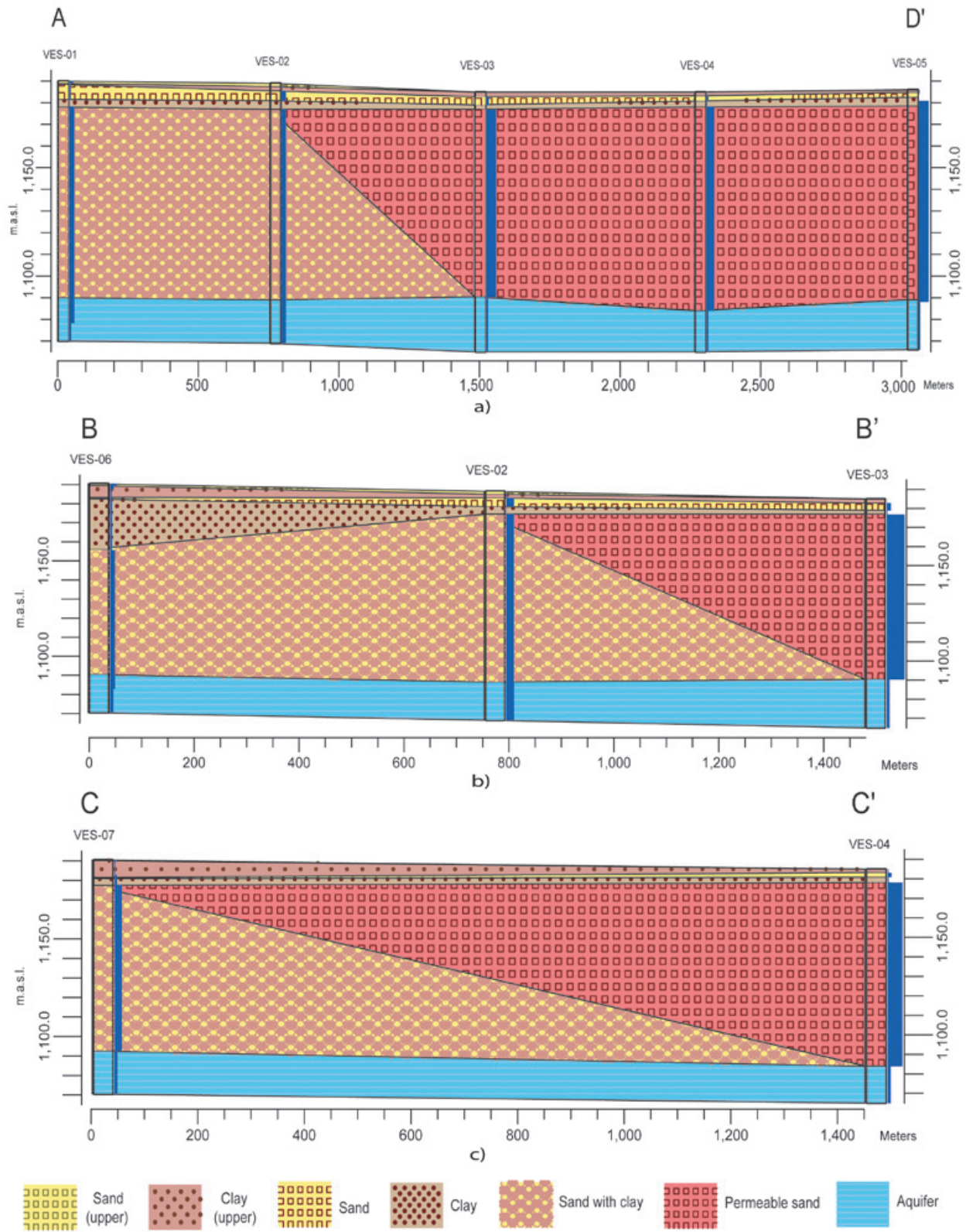
Figure 15. Geoelectric stratigraphic profiles. The legend explains the interpreted stratigraphic horizons. The "upper" units are younger strata. The blue columns represent the 1D inverted models, the widthe are proportional to the inverted resistivity value. a) Profile A-D'. b) Profile B-B'. c) Profile C-C'. For profile location see Figure 1(b).
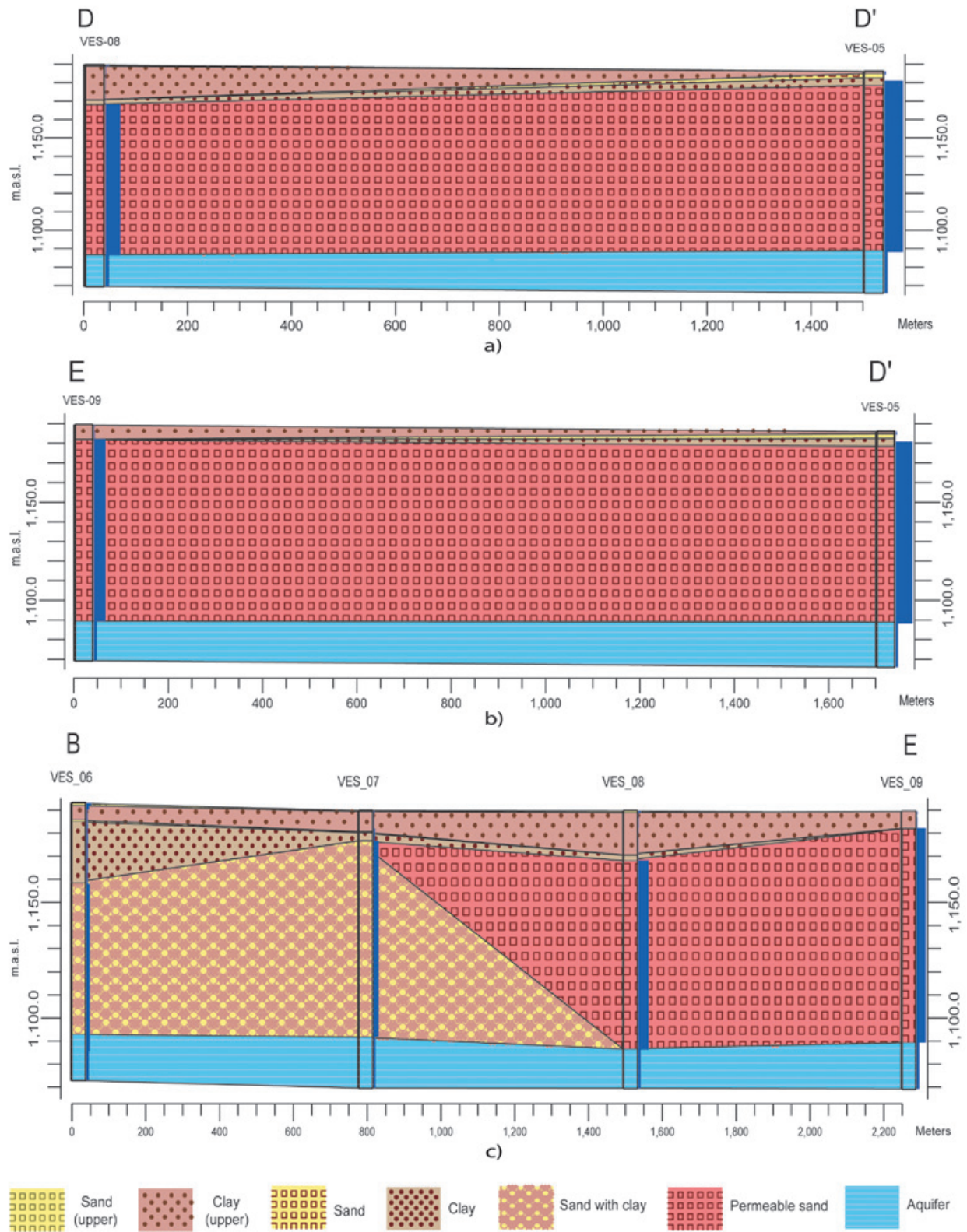
Figure 16. Geoelectric stratigraphic profiles. The legend explains the interpreted stratigraphic horizons. The "upper" units are younger strata. The blue columns represent the 1D inverted models, the widths are proportional to the inverted resistivity value. a) Profile D-D'. b) Profile E-D'. c) Profile B-E. For profile location see Figure 1(b).
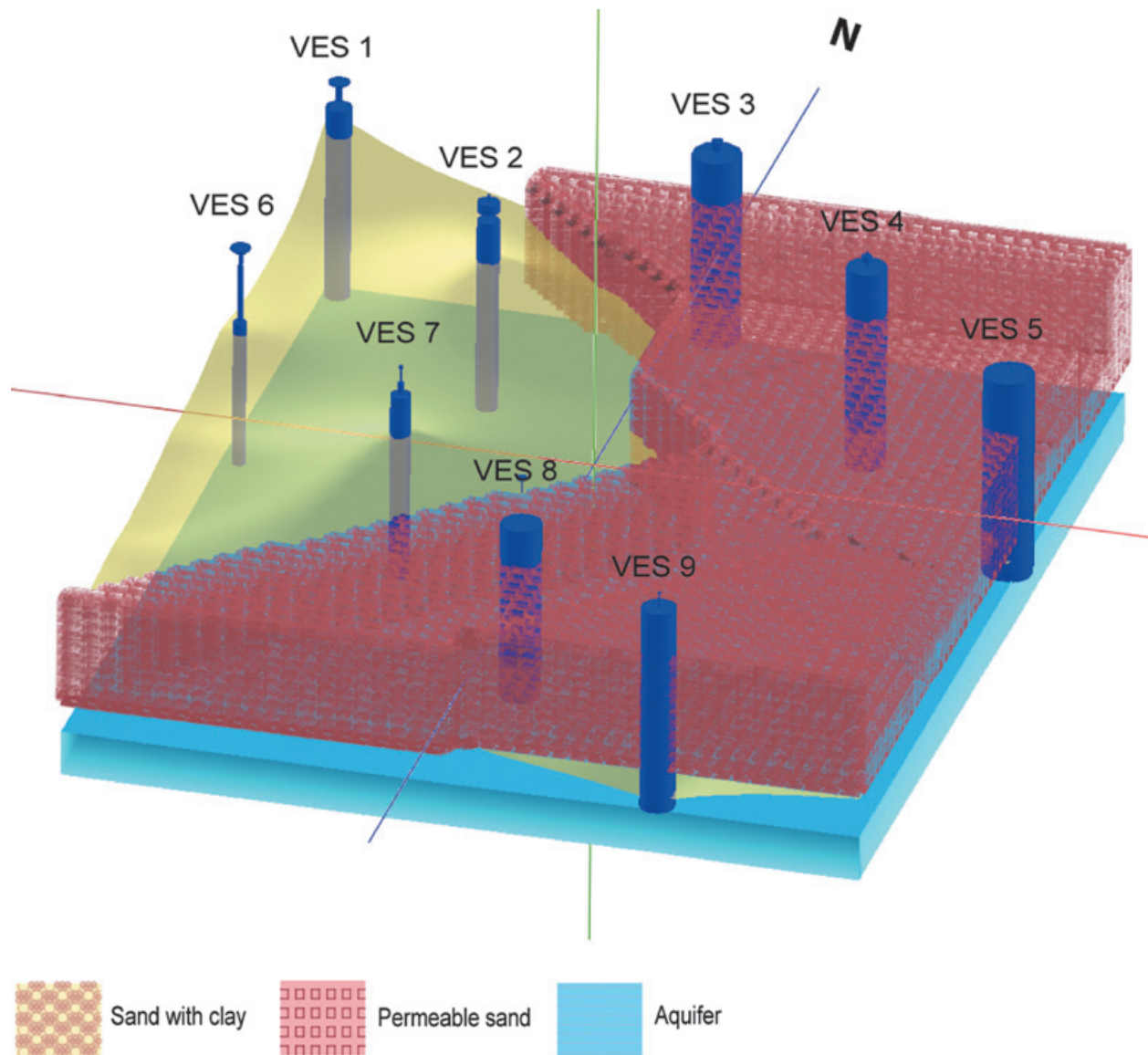
Figure 17. 2D stratigraphic model inferred from geophysics and well data. The widths of the blue columns are proportional to the inverted resistivity value.

Conclusions

The observed lithologies in the trench displayed a good agreement between the modeled resistivity results and the actual underground stratigraphy. However, the main observed disagreement was the presence of fine-grained sand interbedded with a lacustrine sequence, which was initially modeled in the resistivity studies as a single unit. The poor functioning of the absorption wells might suggest they were drilled to a depth that only reached the upper boundary of this fine-grained sand body. Once the observed lithologic units were input as a starting model into the modeling software, a reasonable fit between the theoretical and the observed curves was obtained (Figures 9 to 11). This is not surprising, since several combinations of resistivity impedances can yield the same result (Telford *et al*., 1995; Sharma 1997). It is also true that it is very difficult to infer the true underground structure from a single geophysical technique. Nevertheless, the high resistivity layer (greater than 160 ohm-m and nearly 80 m in thickness) was confirmed to be a relatively permeable (2.45 m/d) sand body suitable to for infiltration.
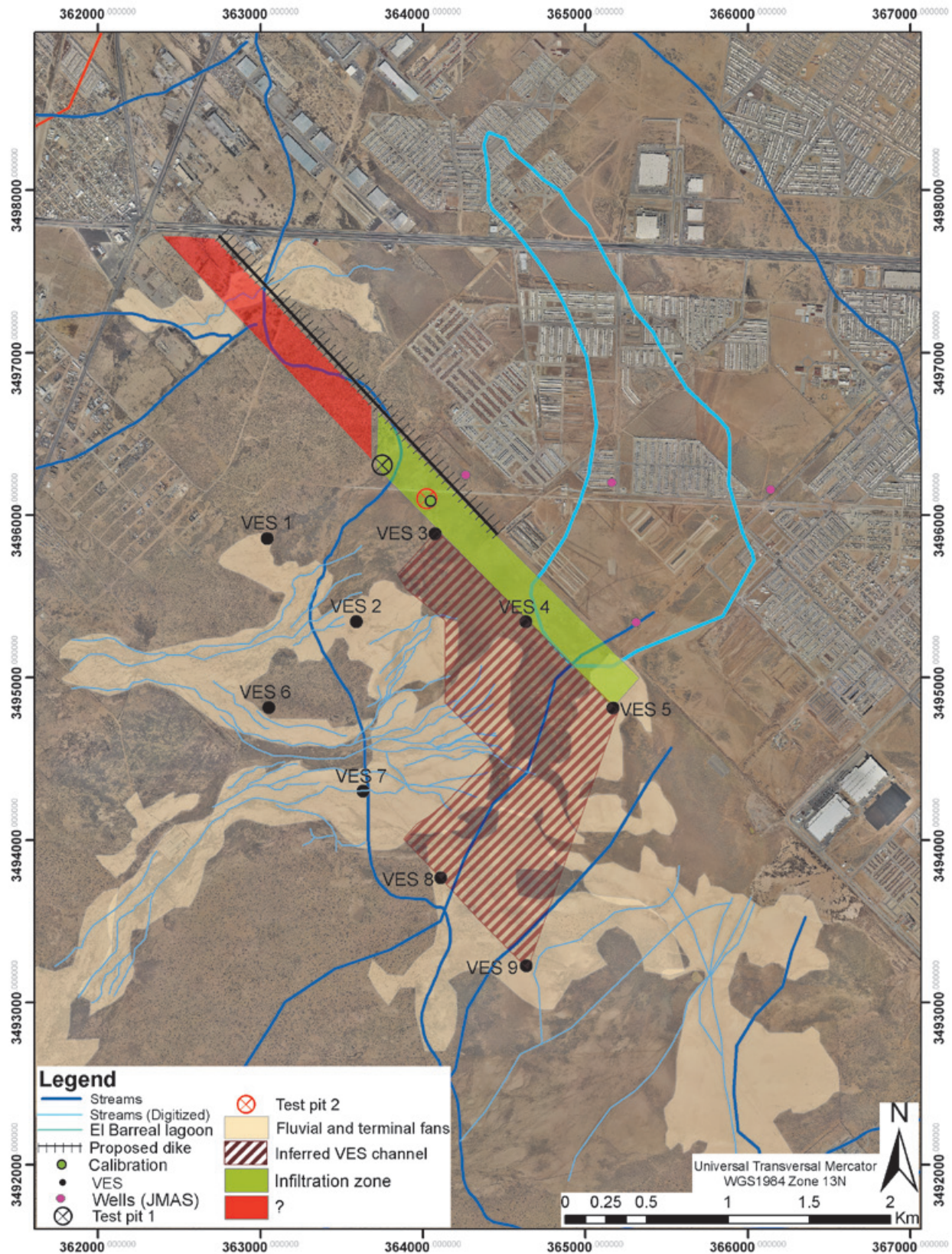
Figure 18. Hydrostratigraphic local scale zoning overlaying 1m pixel size aerial photo. Aerial photo inferred streams are shown in light blue. The green area represents an appropriate infiltration zone in terms of the research results.

We conclude that the DC method was an excellent approach to discriminating between fine and coarse grain materials, however it was limited in resolution. It would be advisable to conduct Electrical Resistivity Tomography (ERT) in the region with an intelligent electrode array capable of yielding profiles with vertical meter resolution. Nevertheless, the DC approach is still an outstanding cost-benefit prospecting tool to provide information on subsurface conditions when tied to existing borehole and other subsurface information. Given the proper subsurface information, this modeling process might reduce the number of direct soundings to only two or three in order to tune the models and generate a final 3D subsurface model with a high degree of certainty.

In terms of our study, our final goal of detecting the depth and extent of a permeable layer in terms of hydrostratigraphic units (H.S.U.) was achieved after integrating the geophysical findings, the remotely sensed and interpreted geomorphology, and a proper geological model into a GIS. This resulted in a bimodal zoning map, which defines the geographical extent of the infiltration prone area (green polygon in Figure 18). Nevertheless, a considerable number of extra DC soundings and/or TDEMs accompanied by ERT profiling are still required to effectively design the entire well infiltration battery with enough capacity to channel surface water into subsurface permeable units in order to provide a feasible solution for the flooding problem in El Barreal zone.

Bibliography

ABEM, 1993, ABEM Terrameter SAS 300 C: Instruction Manual, NO. JN/9006/9138 5000 12, 64 pp.

Allen D.B., 2005, Ice age lakes in New Mexico, New Mexico Museum of Natural History and Science Bulleting, 28, p. 107 – 114.

Averill M.G., 2007, A lithospheric investigation of the southern Río Grande Rift, ETD Collection for University of Texas, El Paso, *http://digitalcommons.utep.edu/dissertations/AAI3273992.*

Burgos A., 1993, A gravimetric study of the thickness of the unconsolidated materials in the Hueco Bolson aquifer, Juárez area, Chihuahua Mexico. M.S. thesis, The University of Texas at El Paso, 80 pp.

Buro Nacional Inmobiliario, 2009, Quieren construir en zona inundable del Barreal, <http://www.buroinmobiliario.com.mx>

Castiglia P.J., Fawcett P.J., 2006, Large Holocene lakes and climate change in the Chihuahuan Desert. Geology (Boulder), 34, 2, p.113-116.

Comisión Nacional del Agua (CNA), 2008, Estudio de Factibilidad para el control integral de avenidas en las cuencas Zona I-Anapra y zona II-Centro en Ciudad Juárez, Chihuahua, Reporte Técnico Final, 255 pág.

Dena O., 2000, Geophysical properties of soils in the upper Río Grande Valley near El Paso, Texas, Department of Geological Science, University of Texas at El Paso, Thesis, 113 pp.

Dena O.S., 2007, Estudio gravimétrico aplicado a prospección de aguas subterráneas al suroeste de Ciudad Juárez, Reporte Técnico Final, Universidad Autónoma de Ciudad Juárez, 68 pág.

Doser D.I., Dena-Ornelas O.S., Langford R.P., Baker M.R., 2004, Monitoring of the yearly changes in the electrical properties of the shallow subsurface at two sites near the Río Grande, west Texas, Journal Envir. and Engineer. Geophysics 9, 179-190.

Granillo J.A., 2004, A gravimetric study of the structure of the northeast portion of the Hueco Bolson, Texas employing GIS Technology. M.S. thesis, The University of Texas at El Paso, 141 pp.

Haenggi W., 2002, Tectonic history of the Chihuahua trough, Mexico and adjacent USA, Part II: Mesozoic and Cenozoic, Mexican Geological Society Bulletin No. LV-1, p. 38-94.

Hawley J.W., 1969, Notes on the geomorphology and the late Cenozoic geology of northwestern Chihuahua: New Mexico Geological Society, 26th Annual Field Conference, Guidebook, p. 131-142.

Hawley J.W., 1993, Geomorphic setting and late Quaternary history of pluvial-lake basins in the southern New Mexico region. New Mexico Bureau of Mines and Mineral Resources, open-file report 391. p. 28.

Hawley J.W., Hibbs B.J., Kennedy J.F., Creel B.J., Remmenga M.D., Johnson M., Lee M.M., Dinterman P., 2000, Trans-International Boundary aquifers in southwestern New Mexico: New Mexico Water Resources Research Institute, New Mexico State University, prepared for U. S. Environment Protection Agency-Region 6 an International Boundary and Water Commission; Technical Completion Report-Interangency Contract X-996350-01-3, 126 p.

Hawley J.W., Hibbs B.J., Kennedy J.F., Creel B.J., 2001, the Mesilla Basin aquifer system of New Mexico, West Texas and Chihuahua –an overview of its hydrogeology framework and related aspects of Aquifers of West Texas: Texas Water Development Board Report 356, p. 76-99.

Instituto Municipal de Investigación y Planeación (IMIP), 2004, Plan Sectorial de Manejo de Agua Pluvial, 384 pág.

Instituto Municipal de Investigación y Planeación (IMIP), 2004b, Plan Parcial El Barreal y Oriente San Isidro, 190 pág.

Juárez Press, 21 de Julio del 2008. No cumplen con ordenamientos para evitar inundaciones, Juárez Press Periodismo Activo, 27 de Marzo del 2010 <http://www.juarezpress. com/n/227.htm>

Keaton J.R., Barnes J., 1996, Paleoseismic Evaluation of the East Franklin Mountains Fault, El Paso, Texas: Final Report, under award, U. S. Geological Survey, National Earthquake Hazards Reduction Program, Program Element III, 1434-94-G-2389.

Keller G.R., Baldridge S.W., 1999, The Río Grande Rift: A geological and geophysical overview, Rocky Mountain Geology, 34, 1, p. 121-130.

Keller G.R., Morgan P., Seager W.R., 1990, Crustal structure, gravity anomalies, and heat flow in the southern Río Grande rift and their relationship to extensional tectonics, in Technophysics, 174, p. 21 - 37.

Kernodle J.M., 1992, Summary of U.S. Geological Survey ground-water-flow models of basins-fill aquifers in the southwestern alluvial basins region. Colorado, New Mexico, and Texas: U.S. Geological Survey, Open-file Report 90-361, 81 p.

Khatun S., Doser D.I., Imana E.C., Keller G.R., 2007, Locating faults in the southern Mesilla Bolson, west Texas and southern New Mexico using 3-D modeling of precision gravity data, J. Envir. and Engineer. Geophys. 12, 149-161.

Knowles D.B., Kennedy R.A., 1956, Groundwater resources of the Hueco Bolson, northeast of El Paso, Texas: Texas Board Water Engineering Bull. 5615-265 p.

Laboratorio de Climatología y Calidad del Aire (LCCA), 2008, Pluviometric records digital database, Departamento de Ingeniería Civil y Ambiental, Universidad Autónoma de Ciudad Juárez (UACJ).

Loke M.H., 2004, TUTORIAL: 2-D and 3-D electrical imaging surveys. www.geoelectrical. com, pp.29-31

McCalpin J.P., 2006, Quaternary faulting and Seismic source Characterization in the El Paso-Juarez Metropolitan Area; Collaborative Research with the University of Texas at El Paso, Program Element II: Evaluate Urban Hazard and Risk, final Technical Report, National Earthquake Hazards Reduction Program U. S. Geological Survey.

Obeso G.J., 2008, Estudio gravimétrico aplicado a prospección de aguas subterráneas al suroeste de Ciudad Juárez. B.S. thesis, Universidad Autónoma de Ciudad Juárez, 70 pág.

O'Donnell T.M., 1998, Integrated gravity seismic reflection/refraction study of the McGregor geothermal system, southern New Mexico. M. S. thesis, University of Texas at El Paso, 142 pp.

Palacky G.I., 1987, Resistivity characteristics of geological targets. In: M. Nabighian, Editor, Electromagnetic Methods in Applied Geophysics-Theory, Society of Exploration Geophysicists, Tulsa, OK, pp.53-129.

Rascón E.M., Gómez F.J., 2007, Estudio de Prospección Geofísica para la ubicación de una fuente de abastecimiento para el nuevo campus de Ciudad Universitaria, al sur de Ciudad Juárez. Reporte Interno Final, Junta Municipal de Agua y Saneamiento (JMAS), 39 pág.

Rascón E.M., 2008, Chief of Department of Geohydrology, Junta Municipal de Agua y Saneamiento (JMAS) de Ciudad Juárez, pers. comm.

Reeves C.C. Jr., 1969, Pluvial Lake Palomas northwestern Chihuahua, Mexico. New Mexico Geological Society, 20th Annual Field Conference, Guidebook. p. 143 -154.

RockWorks. Earth Science and GIS Software, 2002.*http://www.rockware.com/index.php.*

Sayre A.N., Livingston P., 1945, Groundwater resources of the El Paso area, Texas, U.S. Geological Survey Water Supply Paper 919, 190 pp.

Seager W.R., 1980, Quaternary Fault Systems in the Tularosa and Hueco Basins, Southern New Mexico and West Texas, in Guidebook of the Trans Pecos Region: New Mexico Geological Society, 5 pp.

Seager W.R., Morgan P., 1979, Río Grande rift in southern New Mexico, west Texas, and northern Chihuahua. In R.E. Riecker (Editor), Río Grande rift: Tectonics and magmatism. American Geophysical Union, Washington, D.C., pp. 127-143.

Servicio Geológico Mexicano (SGM), 2008, Carta Magnética de Campo Total Escala 1:50,000 de Ciudad Juárez, Chihuahua.

Sharma P.V., 1997, Environmental and engineering geophysics , Cambridge University Press, p. 475, ISBN: 0-521-576326.

Shevnin V.A., Modin I.N., 2003, IPI2win, Program for 1D automatic and manual interpretation of VES curves, Moscow State University, Geological Faculty, Department of Geophysics.

Shevnin V.A, Delgado Rodríguez O., Mousatov A., Nakamura Labastida E., Mejía Aguilar A., 2003, Oil Pollution using resistivity sounding, Geofísica Internacional, 42, 4, pp. 613-642.

Sinno Y.A., Daggett P.H., Keller G.R., Morgan P., Harder S.H., 1986, Crustal structure of the southern Río Grande rift determined from seismic refraction profiles: Journal of Geophysical Research, 91, p. 6143-6156.

Telford W.M., Geldart L.P., Sheriff R.E., 1995, Applied geophysics, Second Edition, Cambridge University Press, p. 751, ISBN: 0-521-33938-3.

Uphoff T.J., 1978, Subsurface stratigraphy and structure of the Mesilla and Hueco Bolsons, in the El Paso Region, Texas and New Mexico: MS Thesis, University of Texas at El Paso 66, p.

Wessel P., Smith W.H.F., 1988, Generic Mapping Tools (GMT), http://gmt.soest.hawaii.edu/, School of Ocean and Earth Science and Technology, University of Hawaii at Manoa.